

X-ray diffraction and equation of state of solid neon to 110 GPa

R. J. Hemley, C. S. Zha,* A. P. Jephcoat, H. K. Mao, and L. W. Finger
Geophysical Laboratory, Carnegie Institution of Washington, Washington, D.C. 20008

D. E. Cox

Department of Physics, Brookhaven National Laboratory, Upton, New York 11973

(Received 11 October 1988)

Solid neon was compressed under static conditions at 300 K to pressures in the 100 GPa (megabar) range using diamond-anvil cell techniques. The crystal structure and P - V equation of state were determined by energy-dispersive x-ray diffraction with microcollimated synchrotron radiation. Pressures were determined from ruby fluorescence spectra and from x-ray diffraction of tungsten powder contained within the sample. Solid neon remains an insulator with the fcc structure to the maximum pressure of 110 GPa at 300 K, where the compression V/V_0 is 0.28. The 300-K P - V isotherm measured at high pressure is in excellent agreement with the results of electronic structure calculations but is incorrectly described by pure pair potentials recently developed for neon. These results indicate that there is a significant softening of the material by many-body interactions at high pressures. Finally, the measurements of ruby fluorescence and tungsten x-ray diffraction in the neon medium obtained in this study provide an extension of the quasihydrostatic ruby pressure scale above 100 GPa.

I. INTRODUCTION

The properties of condensed gases at high pressures continue to attract much experimental and theoretical attention since these materials provide critical tests of theories of bonding in solids.¹⁻⁷ Recent developments in static high-pressure techniques based on the diamond-anvil cell have added a new dimension to this effort. Optical studies of the diatomic solids hydrogen and nitrogen, which have now been performed at pressures above 100 GPa, indicate the occurrence of phase transitions and provide constraints on the structure of the molecular phases at higher pressures.^{2,3} Parallel to these optical studies has been the development of high-pressure x-ray diffraction techniques for direct crystal structure determination. Detailed structural studies of condensed gases at high pressure have proved difficult using conventional diffraction methods owing to the small amounts of material contained in the high-pressure cell under these conditions. Nevertheless, unit-cell parameters for solid argon have been obtained to 80 GPa by conventional polycrystalline x-ray diffraction techniques.⁴ The recent development of techniques for utilizing bright synchrotron x-ray sources for diffraction measurements on high-pressure samples has extended the range of such measurements, particularly for low- Z materials. These techniques now permit the measurement of both single-crystal and polycrystalline x-ray diffraction on condensed gases at very high densities.⁵⁻⁷

One of the significant results of these recent high-pressure x-ray diffraction measurements of condensed gases has been a renewed interest in the crystal structure problem in the rare-gas solids.¹ Using techniques originally developed for high-pressure x-ray diffraction of

solid hydrogen,⁵ the crystal structure of solid helium⁶ was determined by single-crystal synchrotron methods at 15–23 GPa and 300-K. This experiment demonstrated that solid helium crystallizes in the hexagonal-close-packed structure over this P - T range, in contrast to theoretical predictions and indirect experimental studies (see Ref. 6). The earlier polycrystalline x-ray diffraction measurements demonstrated that solid argon remains in the cubic-close packed structure to at least 80 GPa.⁴ More recent synchrotron x-ray diffraction measurements on solid xenon to 137 GPa, on the other hand, demonstrate that the material undergoes a sequence of pressure-induced phase transformations in this pressure range, transforming from the cubic-close-packed structure to an intermediate phase beginning at 14 GPa, and finally to the hexagonal-close-packed structure at 75 GPa.⁷

In addition to new information on pressure-induced polymorphism in the rare-gas solids, these studies have provided useful data on P - V equations of state. The equation of state, in addition to being an important thermodynamic property, provides constraints on the form of the interatomic potential and the contribution of many-body forces at high compressions. Calculations carried out using accurate pair potentials for helium⁴ and argon,⁶ for example, suggest a significant increase in compressibility due to attractive many-body forces at high densities, although the explicit form of the many-body contributions is not yet known. Empirically determined potentials, which implicitly contain many-body terms appropriate for the condensed phase, have been developed to fit the high-pressure data. As a result of their simple form, these potentials are convenient for use in high-temperature simulations for fluids, including multicomponent mixtures. The effective pair potentials developed

for helium and argon successfully describe both the static and shock-wave compression data, which covers a large temperature range from 300-K to greater than 10 000-K, although the pressure range over which the models accurately fit the static x-ray data is somewhat limited.^{4,6}

The behavior of neon at high densities has been the subject of comparatively few experimental and theoretical investigations in relation to studies of other rare-gas solids. Early high-pressure studies of solid neon, cryogenic measurements at pressures limited to below 2.0 GPa, provided information on the thermodynamic properties in the low P - T range (see Ref. 8). Hazen *et al.*⁹ showed that fluid neon freezes at 4.7 GPa and 293 K to form a single crystal in a diamond-anvil cell; the crystal structure and P - V equation of state were subsequently determined from the freezing pressure to 14.4 GPa using single-crystal x-ray diffraction with a conventional four-circle diffractometer.^{9,10} The crystal structure was shown to be cubic-closed packed in this P - T range. The only experimental data on neon at higher pressures have been obtained from high-temperature, dynamic compression experiments. Hawke *et al.*¹¹ reported that adiabatically compressed neon remains an insulator to several hundred GPa; however, pressures achieved in these experiments are highly uncertain since they were not measured but had to be calculated from theoretical considerations.

Information on the properties of neon at higher pressures has largely been obtained from theoretical calculations, including both interatomic potential and band-structure calculations. The determination of an accurate Ne-Ne pair potential has been attempted using low-pressure experimental data for the gas and Hartree-Fock results for the repulsive wall.^{12,13} These calculations have been fraught with difficulties, however, as discussed by Aziz.¹³ In addition, calculations of the Ne-Ne repulsive potential using Gordon-Kim techniques have not been entirely satisfactory.¹⁴ As a result of this uncertainty in the two-body forces, there does not yet appear to be a consensus on the many-body contribution in the solid at high compression. Band-structure methods have been used to calculate properties of the solid at ultrahigh pressures.¹⁵⁻¹⁷ Recent calculations predict that the pressure-induced insulator-metal transition may occur at the highest pressure of any solids considered so far, i.e., in the 100 TPa range. The results suggest that the electronic structure may be only weakly perturbed by pressure at 100 GPa.

In this study we have measured x-ray diffraction of solid neon to 100 GPa to determine its crystal structure and P - V equation of state. Pressures were determined from ruby fluorescence spectra and from x-ray diffraction of tungsten powder contained within the sample. The large compression of neon over this pressure range provides an important test of theoretical models of this electronically simple system. We have calculated P - V - T equations of state from lattice dynamics using recently determined Ne-Ne pair potentials to assess the role of many-body interactions at high compressions. We find that the measured P - V relations are incorrectly described by equations of state calculated using these (pure) pair potentials but are in excellent agreement with the results of recent

electronic structure calculations. Finally, a cross comparison between the ruby fluorescence and tungsten x-ray diffraction measured in this study provides the first direct test of the quasihydrostatic ruby pressure scale above 100 GPa.

II. EXPERIMENTAL PROCEDURE

Samples were prepared using procedures outlined in detail elsewhere.¹⁸ Neon gas was loaded at high pressure and room temperature in a megabar-type diamond-anvil cell with beveled anvils. The neon was confined within a 80 μm hole drilled into a 0.5 mm thick T301 stainless steel gasket that had been preindented to 40 GPa. The diamonds were beveled at 5°, with an inner flat diameter of 250 μm and a culet diameter of 500 μm . Powdered tungsten and ruby were loaded in the sample chamber of the diamond-anvil cell, which was then mounted in a high-pressure gas-loading apparatus.^{18,19} The apparatus was first pressurized with neon to \sim 100 MPa and then depressurized to 0.1 MPa, a cycle that was repeated three times to purge the cell of residual air. After a final compression to 200 MPa the diamond-anvil cell was sealed. Following removal of the cell from the gas-loading device, the pressure was increased above the freezing pressure of neon (4.7 GPa at room temperature) for transport to the synchrotron source.

The x-ray diffraction was measured at the National Synchrotron Light Source, Brookhaven National Laboratory (beam line X13A, now X7A) operating at 2.5 GeV and 50–120 mA. The incident x-ray beam from the synchrotron was collimated to a width of 20–40 μm , and the diffracted x-ray beam was collected with a Si(Li) detector at \sim 18° 2θ scattering angle, which was calibrated with CeO₂ powder at ambient pressure. The measurements were carried out using energy dispersive x-ray (EDX) diffraction techniques.^{20,21}

Pressures of the sample in the diamond-anvil cell were measured *in situ* by x-ray induced ruby fluorescence.²² With this technique, luminescence of ruby is excited by the incident x-ray beam and the visible light emitted is collected by a microscope objective coupled to a 0.18 m spectrometer with a 600 groove/mm grating that disperses the light onto a multichannel photodiode array. The ruby pressure scale²²⁻²⁵ was used to calculate the pressure from the wavelength shift $\Delta\lambda$ of the R_1 fluorescence peak using

$$P = A/B \{ [1 + (\Delta\lambda/\lambda_0)]^B - 1 \},$$

where $A = 1904$ GPa, $B = 7.665$, and $\lambda_0 = 694.2$ nm (Ref. 25). The pressure was also determined from the x-ray diffraction pattern of the tungsten using the 300-K P - V isotherm reduced from shock-wave measurements.^{26,27} The x-ray measurement provided a cross check on the ruby shift determined by x-ray induced fluorescence and provided a means for examining the reliability of the quasihydrostatic ruby scale above the previous pressure limit of the calibration.²⁵

III. EXPERIMENTAL RESULTS

Energy-dispersive x-ray diffraction patterns of neon and tungsten samples are shown as a function of pressure in Fig. 1. The Ne(111) and Ne(200) lines are observed, in addition to the W(110) and W(200) lines. Similar patterns are observed at all pressures. In the pressure range below 30 GPa, however, we noted an irregular variation in the relative intensities of the two Ne bands with each change in pressure. This effect is attributed to partial recrystallization of neon microcrystals which causes changes in preferred orientation with increasing pressure. A similar

effect was noted in the single crystal x-ray study of neon to 14 GPa.¹⁰ With narrow collimation of the synchrotron beam, it was possible in many measurements (e.g., Fig. 1) to discriminate completely against diffraction from the metal gasket which contaminates the sample diffraction pattern. The lattice parameter and molar volume calculated from the diffraction patterns at each pressure are listed in Table I.

A representative x-ray induced ruby fluorescence spectrum measured at high pressure is shown in Fig. 2. The widths of the peaks shown in the figure are determined from the low resolution of the spectrometer used on the synchrotron beam line. We thus infer that the R_1 and R_2 bands remain well resolved over the entire pressure range of the experiment. This finding suggests that the strength of solid Ne above 100 GPa is sufficiently low that the material can be used as a quasihydrostatic medium over this pressure range. We note that the $R_1 - R_2$ separation increases under pressure (from 28 cm^{-1} at 0.1 MPa to $\sim 40 \text{ cm}^{-1}$ at 110 GPa). At low pressure, this increase is indicative of a uniaxial stress component²⁸; however, a quantitative correlation between this shift and the degree of nonhydrostatic stresses on the ruby at these high pressures has not yet been established.

Figure 3 illustrates the wavelength shift of the ruby fluorescence as a function of pressure calculated from the tungsten isotherm.²⁶ The present data are compared with the quasihydrostatic ruby pressure scale determined to 80 GPa.²⁵ In the previous calibration study, the pressures were determined by x-ray diffraction of Cu and Ag in an argon medium using isotherms calculated from shock-wave measurements. In that study the exponent was found by least-squares fit to be $B = 7.665$. We also compared the earlier nonhydrostatic calibration curve determined without a medium, for which $B = 5.0$ (Ref. 24), and the recently proposed pressure scale based on diamond in a helium medium, for which $A = 1918 \text{ GPa}$ and $B = 11.7$ (Ref. 29).

We find that the new data fall close to the recently determined calibration curve to 80 GPa and thus support its use at higher pressures. The tungsten pressures are systematically higher than the predictions of the ruby scale at higher pressures, but this difference is within the expected error in the tungsten isotherm. The agreement with the earlier quasihydrostatic scale is particularly good in comparison with the other curves. The higher exponent of $B = 11.7$ determined in the diamond scale study appears to be inconsistent with the present data. At 300 K, compressed solid helium remains considerably weaker than neon and argon at high pressures,³⁰ so part of this discrepancy may be associated with residual nonhydrostatic effects in the heavier rare-gas media. We point out, however, that the diffraction data obtained in the diamond study (consisting of only one single-crystal reflection) were measured only from ambient pressure to 30 GPa, which represents a rather limited range of compression due to the high incompressibility of diamond ($K_0 = 442 \text{ GPa}$). Errors in extrapolated equations of state determined from high-pressure x-ray diffraction measurements carried out over a small compression range can be considerable (see Ref. 31 for a detailed dis-

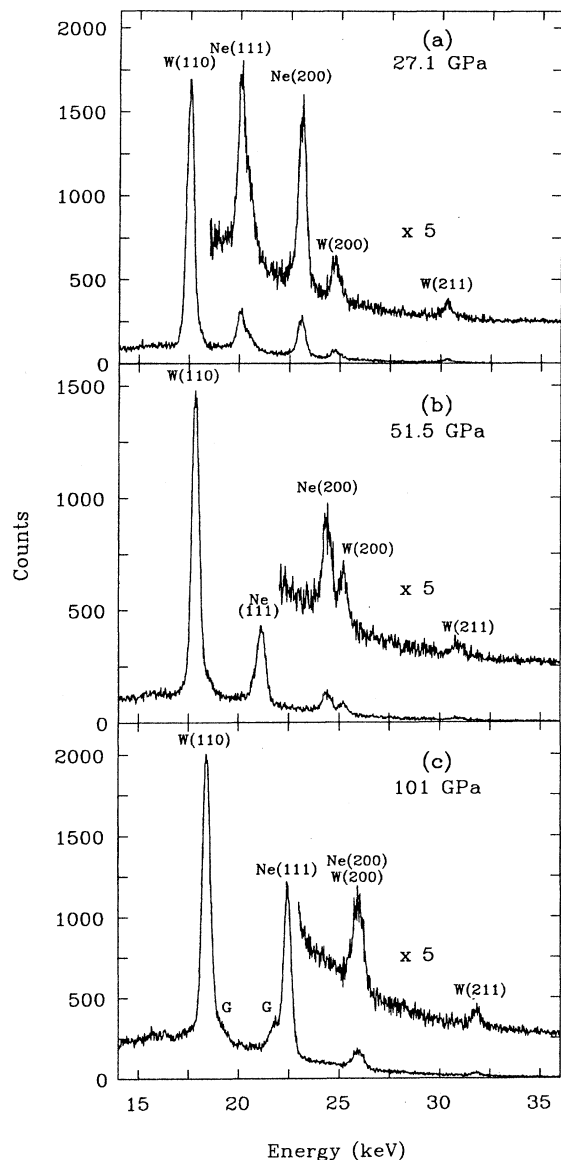


FIG. 1. Energy-dispersive x-ray diffraction patterns of neon and tungsten in a diamond-anvil cell at 300 K as a function of pressure: (a) 27.1 GPa; (b) 51.5 GPa; (c) 101 GPa. The pressures are those determined from the ruby fluorescence measurements. The weak shoulders in the 101 GPa spectra marked G correspond to diffraction from the steel gasket that surrounds the sample.

TABLE I. Lattice parameter and molar volume of fcc neon as a function of pressure to 110 GPa (300 K).

a (Å)	Vol (cm ³ /mol)	P GPa (Ruby)
3.567(±0.010) ^a	6.83(±0.05) ^a	10.0(±0.2) ^b
3.400(±0.010)	5.92(±0.05)	20.0(±0.2)
3.315(±0.010)	5.49(±0.04)	27.1(±0.2)
3.258(±0.010)	5.21(±0.05)	31.0(±0.2)
3.230(±0.010)	5.07(±0.05)	35.6(±0.3)
3.190(±0.010)	4.89(±0.04)	40.3(±0.3)
3.139(±0.010)	4.66(±0.04)	51.5(±0.3)
3.111(±0.010)	4.53(±0.04)	56.9(±0.4)
3.077(±0.010)	4.39(±0.04)	64.4(±0.4)
3.035(±0.010)	4.21(±0.04)	74.3(±0.4)
3.021(±0.010)	4.15(±0.04)	78.3(±0.4)
3.014(±0.010)	4.12(±0.04)	82.3(±0.4)
3.003(±0.010)	4.08(±0.04)	83.5(±0.4)
2.993(±0.010)	4.04(±0.04)	87.5(±0.4)
2.986(±0.010)	4.01(±0.04)	91.1(±0.4)
2.973(±0.010)	3.96(±0.04)	94.5(±0.4)
2.963(±0.010)	3.92(±0.04)	97.7(±0.4)
2.956(±0.010)	3.89(±0.04)	101.0(±0.5)
2.946(±0.010)	3.85(±0.04)	103.7(±0.5)
2.936(±0.010)	3.81(±0.04)	107.7(±0.5)
2.927(±0.010)	3.76(±0.04)	110.4(±0.5)

^aThe principal uncertainties in the lattice parameters and molar volumes are due to the uncertainty in the angle calibration for the energy dispersive x-ray diffraction measurements. A secondary source of error arises from the uncertainty in fitting the x-ray peak positions.

^bThe uncertainties in the pressures are determined largely from the resolution of the R_1 ruby fluorescence peaks and from the error in the wavelength calibration of the optical spectrometer.

cussion of this problem). Higher pressure diffraction measurements are thus required to check these results.

IV. EQUATION OF STATE

The molar volume calculated from the diffraction pattern is plotted as a function of pressure in Fig. 4 along with the results of the earlier single-crystal study at low pressure. Very good agreement with the earlier study is indicated. The results of a least-squares fit using a third-order Birch-Murnaghan finite-strain equation of state³² published previously³³ are compared with experimental results in Fig. 4. The fit was performed by first reducing the 300-K data to 0 K in order to use the low-temperature zero-pressure volume V_0 and bulk modulus K_0 in the fit. The temperature reduction is accomplished

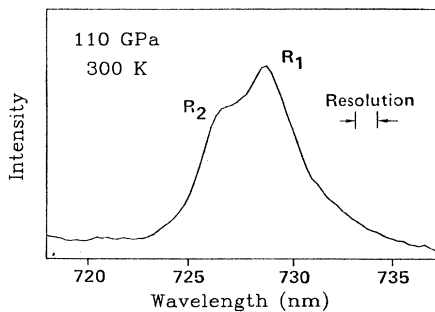


FIG. 2. X-ray induced R_1 and R_2 fluorescence spectrum of ruby in neon at 110 GPa and 300 K.

by the use of a Mie-Grüneisen model³⁴ for the zero-point and thermal pressures (P_{ZP} and P_{TH}). These terms were calculated in the Debye approximation, with

$$P_{ZP} = (9\gamma/8V)R\Theta(V)$$

and

$$P_{TH} = (3RT\gamma/V)D(\Theta/T)$$

where R is the gas constant, Θ is the Debye temperature,

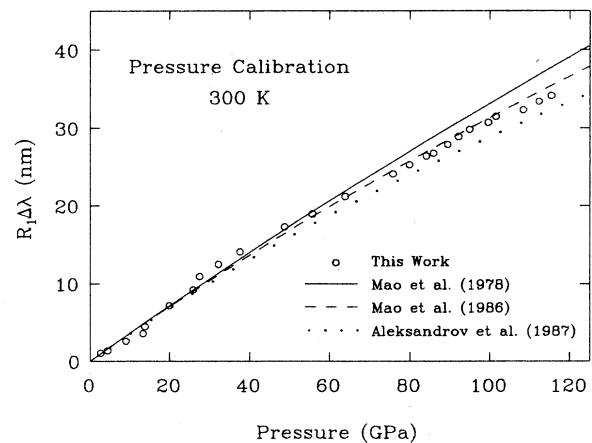


FIG. 3. Wavelength of the ruby fluorescence as function of pressure calculated from the x-ray diffraction and equation of state of tungsten at 300 K.

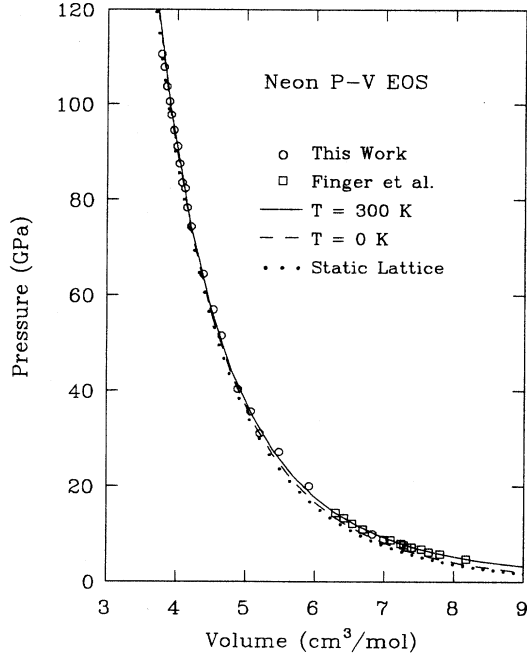


FIG. 4. Pressure-volume equation of state (EOS) of solid neon. The curves represent fits to the experimental high-pressure polycrystalline (300 K) and low-pressure single-crystal (293 K) (Ref. 10) diffraction data using a third-order Birch-Murnaghan finite-strain expansion and a Mie-Grüneisen thermal model.

D is the Debye function, and γ is the Grüneisen parameter, defined as $\gamma = -d \ln \Theta / d \ln V$. The logarithmic volume derivative of γ is $q = d \ln \gamma / d \ln V$. We used the volume dependence of γ from the previous neon study¹⁰: $\gamma = (V/V_0)\gamma_1 + \frac{1}{2}$ (i.e., $q = 1$) with $\gamma_1 = 2.05$. As a check on this, the parameters were also calculated from the second Debye moment of the phonon density of states $\Theta(2) = (5 \langle \omega^2 \rangle / 3)^{1/2} h / k_B$ from lattice dynamics using the exp-6 pair-potential model described below. The latter calculation gave $\gamma = 2.54$ and $q = 0.9$ at zero pressure, which also is consistent with calculations performed using model potentials.³⁵ The $T = 0$ K isotherm $P(V, 0 \text{ K}) = P_S(V) + P_{ZP}(V)$ was then fit to a Birch-Murnaghan equation of state,

$$F(f) = P / [3f(1+2f)]^{5/2} = K_0(1 + af + bf^2 \dots),$$

where F is a normalized stress, f is the strain, defined as $f = \frac{1}{2}[(V_0/V)^{3/2} + 1]$, and K_0 is the zero-pressure bulk modulus. The coefficients of the expansion are given as

$$a = \frac{3}{2}(K'_0 - 4)$$

and

$$b = 2/3K_0K''_0 + 2/3K'^2_0 - 63/6K'_0 + 143/6,$$

where K'_0 and K''_0 are the first and second pressure derivatives of the zero-pressure bulk modulus. The complete set of room-temperature data were fit by least-squares using both linear (third-order) and quadratic (fourth-order) finite-strain expansions with the zero-pressure volume and bulk modulus determined at $T = 4$

K ($V_0 = 13.394 \text{ cm}^3/\text{mol}$ and $K_0 = 1.097 \text{ GPa}$, Ref. 8). With these parameters, it was noteworthy that a third-order expansion ($b = 0$) was sufficient to fit all the data from 4.7 to 110 GPa, with $K'_0 = 9.23(\pm 0.03)$.

As an alternative to the phenomenological equation of state, we also consider the use of pair potential models for the solid. In these calculations the thermal contribution was determined explicitly by quasiharmonic lattice dynamics. The Helmholtz free energy is given as

$$F(V, T) = \Phi(V) + \frac{1}{2} \sum_i \hbar \omega_i(V) + k_B T \sum_i \ln \{ 1 - \exp[-\hbar \omega_i(V)/k_B T] \},$$

where the static-lattice energy $\Phi(V)$ and harmonic normal mode frequencies ω_i are determined from the pair potentials and are summed over 2048 k-points in the Brillouin zone. The equation of state is determined by differentiating the free energy with respect to V at constant T . At lower pressures, it is known that triple-dipole dispersion terms have a non-negligible influence on condensed-phase properties of rare gases.¹ In addition, anharmonicity of the crystal is significant, thus requiring an extended treatment of the lattice dynamics. On the other hand, a number of studies have shown that the harmonic expansion becomes accurate at high pressures (e.g., Ref. 36).

The calculations were performed using three different classes of pair potentials. First, we use empirical potentials that were fit to a variety of experimental gas-phase

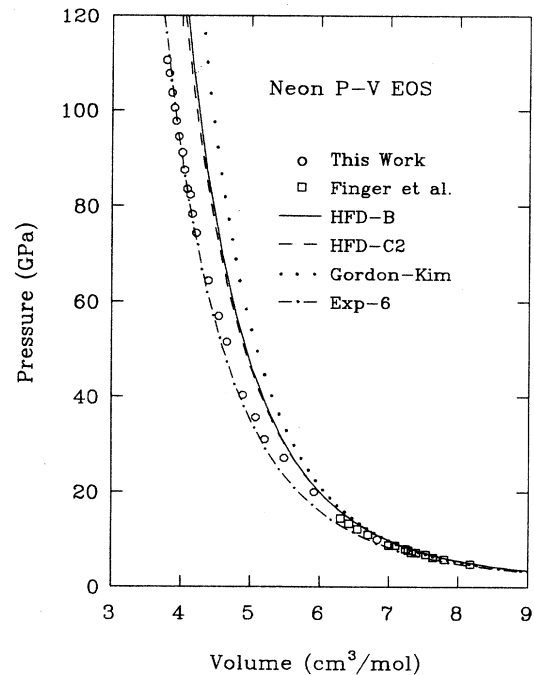


FIG. 5. Comparison of the experimental P - V equation of state (EOS) of neon with the results of lattice-dynamics calculations using recently determined Ne-Ne pair potentials (see the text).

data. These potentials represent the pure two-body Ne-Ne interaction, and are accurate in the region of the attractive well and on the lower portion of the repulsive wall. Here we consider the potential published by Aziz *et al.*¹² as well as the very recent potential of Aziz and Slaman.³⁷ Second, we calculate the Ne-Ne potential from Gordon-Kim (electron-gas) techniques³⁸ using the Hartree-Fock wave function of neon tabulated by Clementi and Roetti.³⁹ Because of the uncertainty in the Gordon-Kim scale factors for neon (see Ref. 14), we consider both unscaled³⁸ and scaled⁴⁰ density functionals. Finally, as an alternative to these *a priori* approaches, we have attempted to fit the P - V data using effective pair potentials. For this we have used an exp-6 potential, a form that has been used with some success in recent analyses of P - V data of helium and argon.^{4,6}

Figure 5 shows the 300-K equations of state calculated from these interatomic potentials. On the scale of the figure, all potentials exhibit good agreement with experiment at low pressures (despite the neglect of triple-dipole and anharmonicity). At higher pressures, however, a significant departure from the predictions of the Aziz and Gordon-Kim pair potential models is observed; i.e., the molar volume (or pressure) is significantly overestimated. For the Gordon-Kim calculation, similar results were obtained using potentials calculated with scale factors and with damped dispersion terms.¹⁴ On the other hand, the figure shows that an effective exp-6 potential can be obtained that fits the experimental data with some success. The parameters of the exp-6 potential used in the calculation shown in the figure are $\alpha = 13.0$, $r_m = 3.14$ Å, and $\epsilon = 42.2$ K. The value for α is within the range of those used in the recent equation-of-state studies of solid helium and argon ($\alpha = 13.0$ – 13.2). As a result, these solids are amenable to calculations using the principle of corresponding states, even to very high densities. Of course, the effective potential includes many-body effects implicitly but no information on the contribution of individual terms. It is apparent that the exp-6 potential is not sufficiently flexible to fit the experimental data over the entire P - V range; i.e., the calculated pressures are too low at low compressions. In addition, the exp-6 is unable to reproduce low-pressure gas-phase properties that are accurately fit by the Aziz-type potentials.

Figure 6 compares the experimental equation of state with results of electronic structure calculations, including predictions for behavior at much higher densities. The isotherm calculated by Zharkov and Trubitsyn¹⁵ was determined by interpolation between the quantum statistical results for the terapascal range and the early experimental data at low pressures (< 2 GPa).⁸ The equation of state determined by Hama¹⁶ was obtained using local density methods; it converges with quantum statistical result in the 1000 GPa (terapascal) range. Both calculations appear to underestimate the pressure above ~ 6 gm/cm³. Boettger¹⁷ calculated the equation of state using local density methods and a Gaussian-type orbital basis. At lower pressure (below 30 GPa) both local density calculations underestimate the pressure, an effect presumably associated with limitations of the method for expanded volumes.¹⁷ The pressures calculated by

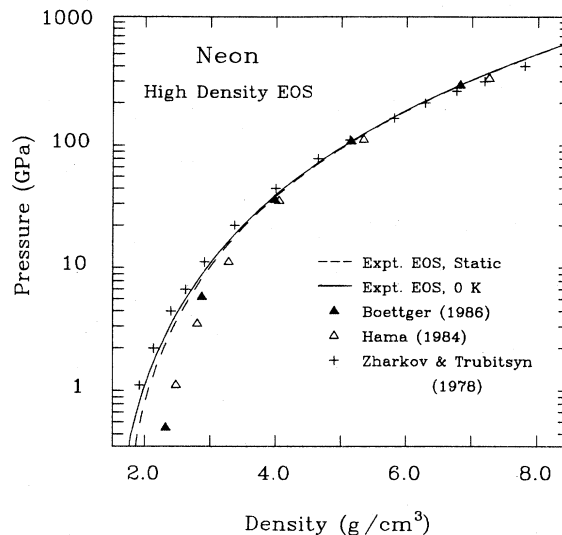


FIG. 6. Comparison of the temperature-reduced ($T=0$ K) and static-lattice P - ρ Birch-Murnaghan equation of state (EOS) with theoretical predictions for neon at high densities. The Hama (Ref. 16) and Boettger (Ref. 17) results are static-lattice calculations (no zero-point pressure); that of Zharkov and Trubitsyn (Ref. 15) is the $T=0$ K isotherm.

Boettger are systematically higher than those determined by Hama. In the high density region, the former are in excellent agreement with the experimental curve (i.e., calculated points at $\rho = 5.15$ gm/cm³, $P = 97$ GPa; and $\rho = 6.82$ gm/cm³, $P = 278$ GPa).

V. DISCUSSION

The present data indicate that solid neon remains in the face-centered cubic structure to pressures above 100 GPa at 300 K. It is useful to contrast the behavior of solid xenon, which transforms to an hexagonal closed-packed structure at 75 GPa; moreover, this solid appears to proceed through an intermediate phase at pressures as low as 14 GPa.⁷ The number of x-ray diffraction peaks is limited in the present measurements, principally as a result of falloff in the x-ray intensity above 30 keV; nevertheless, the neon diffraction peaks remain sharp and well resolved, and there is no broadening of the low-energy fcc peaks observed at the onset of the transformation in xenon. In addition, no significant changes in optical properties were observed. We conclude that the material remains an insulator with a large band gap over the P - T range of the measurements.

The equations of state calculated from pure potentials uniformly overestimate the volume (or pressure) of neon at high pressures. A similar conclusion was reached for solid helium⁶ on the basis of a comparison of single-crystal x-ray diffraction measurements and equation of state calculations; in the helium study a relative compression of $V/V_0 = 0.18$ was achieved. The error in the pair-potential models may reflect inadequacies of the form of the repulsive part of the potentials. Indeed, the determination of the entire potential for neon has been a

difficult problem in the last few years (see Ref. 13). Aziz and coworkers have determined interatomic potentials for rare-gas pairs in the repulsive region from SCF Hartree-Fock calculations; these results are then combined with a semiempirical determination of the potential at long and intermediate range (i.e., near the minimum).¹³ More recent potentials calculated by this group, however, were not fit to Hartree-Fock results for the repulsive wall but were adjusted to fit exchange-Coulomb-type potentials and high-energy molecular beam data.¹² The molecular beam results provide the best estimate of the pure two-body interaction high on the repulsive wall, although the uncertainties are of order 10% (see Ref. 13).

The deviation between the measured high-pressure data and the prediction of the pure pair potential models may be taken as a measure of the effect of many-body forces on the compression of solid. At low densities the leading many-body term is the three-body dispersion or triple-dipole (Axilrod-Teller-Muto) term.¹ Inclusion of this term in the pair-potential calculations would cause a small positive shift in the pressure, thereby worsening the agreement with experiment. Overlap effects on the dispersion terms as a function of compression can be incorporated in an approximate way by scaling both the pair and many-body dispersion terms. As has been shown for compressed argon,⁴¹ the use of such scaling decreases the contribution from the pair and many-body dispersion terms.

As discussed by Meath and Aziz,⁴² at high compressions many-body exchange terms are believed to represent the largest many-body contribution. This con-

clusion is supported by the results of SCF calculations⁴³⁻⁴⁵ and earlier Gordon-Kim results⁴⁶ for the isolated Ne₃ cluster. Recent calculations for other rare-gas solids at high pressure have incorporated these terms.⁴⁷ The extent to which overlap effects will serve to diminish this contribution in the compressed solid, however, is not yet clear.⁴⁸ On the basis of the observed discrepancies between the pure pair-potential models and the experimental *P-V* data, it appears likely that the many-body exchange contribution may be the source of the softening of the repulsive forces. Le Sar⁴⁹ has recently shown that the degree of softening of the helium equation of state needed to bring calculated and experimental data into agreement can be understood in terms of compression of charge density of the component atoms; the magnitude of this contraction was predicted using a many-body model based on nonempirical Gordon-Kim techniques. This approach appears to be applicable to other rare-gas solids as well.⁴¹

ACKNOWLEDGMENTS

We thank R. A. Aziz for communicating results prior to publication and R. E. Cohen and D. E. Townsend for useful discussions. This research was supported in part by the Carnegie Institution of Washington, the U. S. National Science Foundation (Grant No. EAR-8419982) and NASA (Contract No. NAGW-214), and the U.S. Department of Energy, Division of Materials Research (Contract No. DE-AC-2-76CH00016). The National Synchrotron Light Source, Brookhaven National Laboratory, is supported by U.S. Department of Energy, Division of Materials Sciences and Division of Chemical Sciences.

*Present address: Center for Fundamental Physics, University of Science and Technology of China, Hefei, Anhui, The People's Republic of China.

¹M. Klein and J. Venables, *Rare Gas Solids* (Academic, New York, 1976), Vol. 1.

²H. K. Mao, P. M. Bell, and R. J. Hemley, *Phys. Rev. Lett.* **55**, 99 (1985); R. J. Hemley and H. K. Mao, *ibid.* **61**, 857 (1988).

³R. Reichlin, D. Schiferl, S. Martin, C. Vanderborgh, and R. L. Mills, *Phys. Rev. Lett.* **55**, 1464 (1985); P. M. Bell, H. K. Mao, and R. J. Hemley, *Physica* **139&140B**, 16 (1986); R. J. Hemley *et al.* (unpublished).

⁴M. Ross, H. K. Mao, P. M. Bell, and J. A. Xu, *J. Chem. Phys.* **85**, 1028 (1986).

⁵H. K. Mao, A. P. Jephcoat, R. J. Hemley, L. W. Finger, C. S. Zha, R. M. Hazen, and D. E. Cox, *Science* **239**, 1131 (1988).

⁶H. K. Mao, R. J. Hemley, Y. Wu, A. P. Jephcoat, L. W. Finger, and C. S. Zha, and W. A. Bassett, *Phys. Rev. Lett.* **60**, 2649 (1988).

⁷A. P. Jephcoat, L. W. Finger, H. K. Mao, D. E. Cox, R. J. Hemley, and C. S. Zha, *Phys. Rev. Lett.* **59**, 2670 (1987).

⁸M. S. Anderson and C. A. Swenson, *J. Phys. Chem. Solids* **10**, 145 (1975).

⁹R. M. Hazen, H. K. Mao, L. W. Finger, and P. M. Bell, *Carnegie Inst. Washington Yearb.* **79**, 348 (1980).

¹⁰L. W. Finger, R. M. Hazen, G. Zou, H. K. Mao, and P. M. Bell, *Appl. Phys. Lett.* **39**, 892 (1981).

¹¹P. S. Hawke, T. J. Burgess, D. E. Duerre, J. G. Huebel, R. N. Keeler, H. Klapper, and W. C. Wallace, *Phys. Rev. Lett.* **40**, 994 (1978).

¹²R. A. Aziz, W. J. Meath, and A. R. Allnatt, *Chem. Phys.* **78**, 295 (1983).

¹³R. A. Aziz, in *Inert Gases*, Vol. 34 of *Springer Series in Chemical Physics*, edited by M. L. Klein (Springer, New York, 1984), pp. 5-86.

¹⁴R. Le Sar, *J. Phys. Chem.* **88**, 4272 (1984).

¹⁵V. N. Zharkov and V. P. Trubitsyn, *Physics of Planetary Interiors* (Pachart, Tucson, Arizona, 1978).

¹⁶J. Hama, *Phys. Lett. A* **105**, 303 (1984).

¹⁷J. C. Boettger and S. B. Trickey, *Phys. Rev. B* **29**, 6425 (1984); J. C. Boettger, *ibid.* **33**, 6788 (1986).

¹⁸A. P. Jephcoat, H. K. Mao, and P. M. Bell, in *Hydrothermal Experimental Techniques*, edited by G. C. Ulmer and H. L. Barnes (Wiley Interscience, New York, 1987), p. 469.

¹⁹R. L. Mills, D. H. Leibenberg, J. C. Bronson, and L. C. Schmidt, *Rev. Sci. Instrum.* **51**, 891 (1980).

²⁰A. P. Jephcoat, H. K. Mao, C. S. Zha, P. M. Bell, L. W. Finger, and D. E. Cox, *Natl. Synchrotron Light Source Annual Report*, 1986, p. 323.

²¹M. A. Baublitz, V. Arnold, and A. L. Ruoff, *Rev. Sci. Instrum.* **52**, 1616 (1981); K. E. Brister, Y. K. Vohra, and A. L. Ruoff, *ibid.* **57**, 2560 (1986).

²²C. S. Zha, H. K. Mao, A. P. Jephcoat, P. M. Bell, R. J. Hem-

- ley, L. W. Finger, and D. E. Cox, *EOS Trans. Am. Geophys. Union* **67**, 1216 (1986).
- ²³G. J. Piermarini, S. Block, J. D. Barnett, and R. A. Forman, *J. Appl. Phys.* **46**, 2774 (1975).
- ²⁴H. K. Mao, P. M. Bell, J. W. Shaner, and D. J. Steinberg, *J. Appl. Phys.* **49**, 3276 (1978).
- ²⁵H. K. Mao, J. A. Xu, and P. M. Bell, *J. Geophys. Res.* **91**, 4673 (1986).
- ²⁶R. G. McQueen, S. P. Marsh, J. W. Taylor, J. N. Fritz, and W. J. Carter, in *High-Velocity Impact Phenomena*, edited by R. Kinslow (Academic, New York, 1970), pp. 293–417.
- ²⁷D. Schiferl, J. N. Fritz, A. I. Katz, M. Schaefer, E. F. Skelton, S. B. Qadri, L. C. Ming, and M. H. Manghnani, in *High-Pressure Research in Mineral Physics*, edited by M. H. Manghnani and Y. Syono (Terra Scientific, Tokyo-American Geophysical Union, Washington, D. C., 1987), pp. 75–83.
- ²⁸A. L. Schawlow, in *Advances in Quantum Electronics*, edited by J. R. Singer (Columbia University, New York, 1961), pp. 50–62.
- ²⁹I. V. Aleksandrov, A. F. Goncharov, A. N. Zisman, and S. M. Stishov, *Zh. Eksp. Teor. Fiz.* **93**, 680 (1987) [*Sov. Phys.—JETP* **66**, 384 (1987)].
- ³⁰P. M. Bell and H. K. Mao, *Carnegie Inst. Washington Yearb.* **80**, 404 (1981).
- ³¹P. M. Bell, H. K. Mao, and J. A. Xu, in *High-Pressure Research in Mineral Physics*, edited by M. H. Manghnani and Y. Syono (Terra Scientific, Tokyo-American Geophysical Union, Washington, D.C., 1987), pp. 447–454.
- ³²F. Birch, *J. Phys. Chem. Solids* **38**, 175 (1977).
- ³³R. J. Hemley, A. P. Jephcoat, C. S. Zha, H. K. Mao, L. W. Finger, and D. E. Cox, in *High Pressure Science and Technology*, Proceedings of the XIth AIRAPT International Conference, Kiev, 1987, edited by N. V. Novikov (Naukova Dumka, Kiev, U.S.S.R., 1989), Vol. 3, pp. 211–217.
- ³⁴W. C. Wallace, *Thermodynamics of Crystals* (Wiley, New York, 1972).
- ³⁵G. H. Wolf and R. Jeanloz, *Phys. Rev. B* **32**, 7798 (1985).
- ³⁶H. J. Pollock, T. A. Bruce, G. V. Chester, and J. A. Krumhansl, *Phys. Rev. B* **5**, 4180 (1972).
- ³⁷R. A. Aziz and M. J. Slaman, *Chem. Phys.* (to be published).
- ³⁸R. G. Gordon and Y. S. Kim, *J. Chem. Phys.* **56**, 3122 (1972).
- ³⁹E. Clementi and C. Roetti, *At. Data Nucl. Data Tables* **14**, 177 (1974).
- ⁴⁰M. Waldman and R. G. Gordon, *J. Chem. Phys.* **71**, 1325 (1979).
- ⁴¹A. P. Jephcoat, Ph.D. thesis, Johns Hopkins University, 1986; A. P. Jephcoat, R. J. Hemley, and R. LeSar (unpublished).
- ⁴²W. J. Meath and R. A. Aziz, *Mol. Phys.* **52**, 225 (1984).
- ⁴³O. Navaro and F. Nieves, *J. Chem. Phys.* **65** 1109 (1976).
- ⁴⁴M. Bulski and G. Chalasinski, *Theor. Chim. Acta (Berlin)* **56**, 199 (1980); M. Bulski, *Chem. Phys. Lett.* **78**, 361 (1981).
- ⁴⁵B. H. Wells and S. Wilson, *Mol. Phys.* **57**, 21 (1986).
- ⁴⁶Y. S. Kim, *Phys. Rev. A* **11**, 796 (1975).
- ⁴⁷P. Loubeyre, *Phys. Rev. Lett.* **58**, 1857 (1987); *Phys. Rev. B* **37**, 5432 (1988).
- ⁴⁸J. A. Barker, *Mol. Phys.* **57**, 755 (1986).
- ⁴⁹R. LeSar, *Phys. Rev. Lett.* **61**, 2121 (1988).